

1,3-Disubstituted-imidazo[1,5-*a*]pyrazines as insulin-like growth-factor-I receptor (IGF-IR) inhibitors

Mark J. Mulvihill,* Qun-Sheng Ji, Doug Werner, Patricia Beck, Cara Cesario, Andrew Cooke, Matthew Cox, Andrew Crew, Hanqing Dong, Lixin Feng, K. W. Foreman, Gilda Mak, Anthony Nigro, Matthew O'Connor, Lydia Saroglou, Kathryn M. Stolz, Izabela Sujka, Brian Volk, Qinghua Weng and Robin Wilkes

(OSI) Oncology, OSI Pharmaceuticals, Inc., 1 Bioscience Park Drive, Farmingdale, NY 11735, USA

Received 28 September 2006; revised 4 November 2006; accepted 7 November 2006

Available online 10 November 2006

Abstract—A series of novel 8-amino-1,3-disubstituted-imidazo[1,5-*a*]pyrazines was designed and synthesized as IGF-IR inhibitors. © 2006 Elsevier Ltd. All rights reserved.

Receptor tyrosine kinases (RTKs) represent a class of growth-factor receptors that serve as important signal regulators for a variety of cellular functions including differentiation, proliferation, and apoptosis. Activation of RTKs by mutations, over-expression and/or auto-crine/paracrine ligand productions leading to constitutive mitogenic and/or survival signaling has been found to play a critical role in neoplastic progression in humans.¹ Within the realm of tyrosine kinase targets for oncology, the insulin-like growth-factor-I receptor (IGF-IR) has emerged as a key oncology RTK target. Stimulation of IGF-IR through binding of either IGF-I or IGF-II ligand leads to receptor autophosphorylation and activation, which, in turn, recruits and phosphorylates downstream intracellular substrates including IRS-1 and Shc.² Activation of intracellular substrates leads to signal transduction processes which operate through both the Ras/Raf/MEK/ERK and PI3K/Akt/mTOR pathways. These downstream pathways synergize to promote cellular proliferation, inhibit apoptosis, and increase cell survival. The correlation between cancer and IGF signaling is supported by epidemiological studies in which increased expression of the receptor and/or its ligands is prevalent in a broad range of solid tumors and hematologic neoplasias.^{2b,d,3} Recent

data from our research efforts as well as others indicate that an active IGF-II autocrine loop may play an important role in colon cancer progression.⁴ Additional research suggests that inhibition of IGF-IR leads to an induction of apoptosis in tumors while producing only growth arrest in untransformed cells; this suggests a potential window for tumor selectivity in therapeutic applications.^{2c} Inhibition of IGF-IR by various approaches, including antisense,⁵ anti-IGF-IR antibodies,⁶ dominant-negative IGF-IR,⁷ and small-molecule inhibitors,⁸ has been shown to reduce tumor growth in human tumor xenograft models with IGF-IR antibodies having progressed into clinical trials.⁹ Two notable preclinical small molecule IGF-IR inhibitors include the pyrrolo-pyrimidine analog NVP-AEW541 and the benzimidazole derivative BMS-554417.^{8a,b}

Our interest in identifying small-molecule IGF-IR kinase inhibitors for therapeutic applications centered around the underexploited imidazo[1,5-*a*]pyrazine core (Fig. 1). This novel 6/5 heteroaryl template retains key pharmacophoric donor/acceptor interactions with the

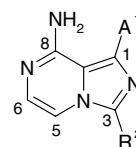


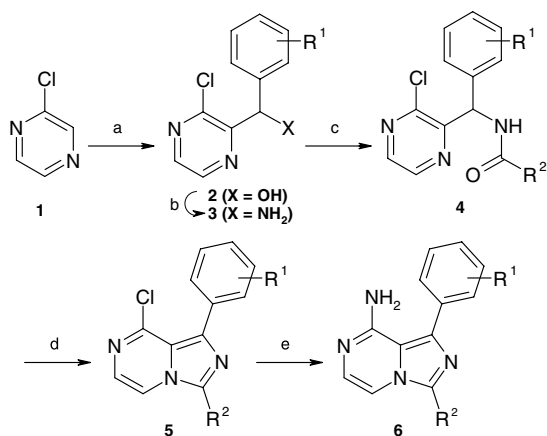
Figure 1. 1,3-Disubstituted 8-aminoimidazopyrazines.

Keywords: IGF-IR; IR; Tyrosine kinase inhibitors; Oncology; Imidazopyrazines; Imidazo[1,5-*a*]pyrazines; Insulin-like growth-factor-I receptor; Insulin receptor.

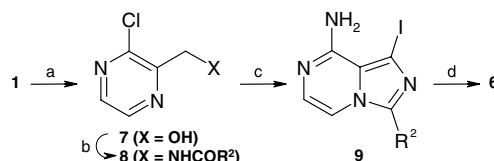
* Corresponding author. Tel.: +1 631 962 0787; fax: +1 631 845 5671; e-mail: mmulvihill@osip.com

kinase hinge region and facilitates efforts to build upon structure–activity relationships established from IGF-IR/IR inhibitors and kinase inhibitors in general, particularly from the thieno-, pyrrolo-, and pyrazolo-pyrimidine series.^{8a,10} This imidazo[1,5-*a*]pyrazine core offers additional advantages over the conventional pyrrolo[2,3-*d*]pyrimidine core, including: a slightly lower polar surface area (PSA), $\log P$, and $\log D$, which increases the flexibility in attachment selection; higher basicity for potentially greater hinge-binding affinity; improved predicted solubilities;¹¹ stable attachment of both carbon and heteroatoms to C3 directly or with a methylene linker. The currently described molecules also enjoy the benefit of (1) synthetic flexibility at C3, where substituents are derived from common carboxylic acids and (2) the inclusion of C1 substituents either in the first step through a linear route or at the last step through a convergent route. As such, we report herein a novel series of 8-amino-1,3-disubstituted-imidazo[1,5-*a*]pyrazines (6) as IGF-IR tyrosine kinase inhibitors.

Two routes, linear and convergent, were employed in order to allow for modifications at C1 and C3 of the imidazopyrazine core.¹² Scheme 1 illustrates the linear route where 2-chloropyrazine (1) underwent a directed *ortho*-metallation in the presence of a preformed solution of lithium tetramethylpiperidide followed by quenching with various aldehydes to afford alcohol 2.¹³ Conversion of alcohol 2 to amine 3 via the Gabriel synthesis proceeded through the Mitsunobu reaction with phthalimide followed by deprotection with hydrazine. Acylation of amine 3 with various acid chlorides ($R^2\text{COCl}$) or through couplings with a variety of carboxylic acids ($R^2\text{CO}_2\text{H}$) afforded amide 4, which, when treated with POCl_3 , cyclized to afford 8-chloroimidazo[1,5-*a*]pyrazine 5. Treatment of compound 5 with ammonia in isopropanol in a Parr reactor at 110 °C for 24 h afforded the desired 8-aminoimidazopyrazine products 6.



Scheme 1. Reagents and conditions: (a) 2 M *n*-BuLi in hexanes, tetramethylpiperidine, –78 °C, then R^1 -Ph-CHO; (b) *i*-phthalimide, DIAD, PPh_3 , THF; ii— NH_2NH_2 , 3:1 EtOH/ CH_2Cl_2 , 16 h; (c) $R^2\text{CO}_2\text{H}$, EDC, HOBT, CH_2Cl_2 or $R^2\text{COCl}$, DIEA, CH_2Cl_2 ; (d) POCl_3 , CH_3CN , 80 °C, 24 h; (e) NH_3 , *i*-PrOH, 110 °C, 24 h.



Scheme 2. Reagents and conditions: (a) 2 M *n*-BuLi in hexanes, tetramethylpiperidine, –78 °C, then DMF, MeOH, and NaBH_4 ; (b) *i*-phthalimide, DIAD, PPh_3 , THF; ii— NH_2NH_2 , 3:1 EtOH/ CH_2Cl_2 , 16 h; iii— $R^2\text{CO}_2\text{H}$, EDC, HOBT, CH_2Cl_2 or $R^2\text{COCl}$, DIEA, CH_2Cl_2 ; (c) *i*- POCl_3 , CH_3CN , 80 °C, ii—NIS, DMF, rt, 16 h; iii— NH_3 , *i*-PrOH, 110 °C, 24 h; (d) $\text{Pd}(\text{PPh}_3)_4$, 4:1 DME/ H_2O , 100 °C, K_2CO_3 , R^1 -Ph-B(OH) $_2$ / R^1 -Ph-B(pin).

Scheme 2 illustrates the convergent route where 2-chloropyrazine (1) underwent a directed *ortho*-metallation as described above, followed by quenching with DMF and subsequent treatment with NaBH_4 in methanol to afford alcohol 7. Conversion of alcohol 7 to its respective phthalimide via the Mitsunobu reaction, followed by deprotection with hydrazine to the amine (Gabriel synthesis), and subsequent acylation, afforded amide 8. Treatment of amide 8 with POCl_3 afforded 8-chloroimidazopyrazine, which, when subjected to NIS followed by ammonolysis, afforded 8-amino-1-iodoimidazopyrazine 9. Compound 9 underwent Suzuki coupling with various arylboronic acids/esters to afford the desired final 1-aryl-8-aminoimidazopyrazines 6.

To determine biochemical inhibitory activity, compounds were tested using a GST-tagged recombinant kinase domain derived from human IGF-IR and assayed using poly (Glu/Tyr) 4:1 as the substrate at an ATP concentration of 100 $\mu\text{mol/L}$. Compounds which displayed biochemical activities below 1 μM were further tested for inhibition of IGF-I-stimulated receptor autophosphorylation in intact cells, where an NIH-3T3 line stably overexpressing full-length human IGF-IR was employed in a capture ELISA.¹²

Table 1. IGF-IR biochemical potencies for compounds 6a

Compound	R^1	IC_{50} (μM)
6a.1	H	>10.0
6a.2	3-OMe	>10.0
6a.3	4-OMe	>10.0
6a.4	3-OBn	0.606
6a.5	4-OBn	1.97
6a.6	3-OH	0.518
6a.7	4-OH	>10.0
6a.8	4-OPh	>10.0
6a.9	3-OBn-4-OMe	1.35
6a.10	3-OBn-4-OH	3.31

Initial synthetic efforts focused on a small subset of substituted phenyls at C1 of the imidazopyrazine (Table 1). In general, 3-substitution was preferred over 4-substitution although both the simple 3- and 4-methoxyphenyls as well as unadorned phenyl were inactive. The 3-benzyloxyphenyl (**6a.4**) and 3-hydroxyphenyl derivatives (**6a.6**) had biochemical IC₅₀ values of 0.606 and 0.518 μM, respectively. However, where the activity of the 3-hydroxyphenyl-derivative **6a.6** was lost in cells, the 3-benzyloxyphenyl derivative **6a.4** retained cellular potency with an IC₅₀ of 1.16 μM. Combining the inactive 4-methoxy- and 4-hydroxyphenyl groups with the preferred 3-OBn tether (compounds **6a.9** and **6a.10**, respectively) allowed recovery of biochemical activity to the low micromolar range.

To facilitate synthetic prioritization, a simple model of the compound class was generated from the published structure of IGF-IR in the Protein Data Bank (pdb), yielding a single kinase domain for IGF-IR (Fig. 2).¹⁴ All amino termini were capped with acetyls and all carboxy termini were capped with amino methyls. After fully protonating the protein, all protein atoms were assigned AMBER7¹⁵ charges in SYBYL (Tripos, St. Louis). The structure of AMPPNP bound to chain 'A'

was modified to correspond to the inhibitor **6a.6** with all protons added; Gasteiger-Huckel charges were then assigned. The torsion between the imidazopyrazine and the phenyl was initialized to 290°. Rotamers for the terminal alcohol, thiol, or amide of cysteines, serines, threonines, tyrosines, asparagines, and glutamines, as well as the tautomers and rotamers of histidines, that generated the best intramolecular protein–protein hydrogen bonds, were selected for all such residues within 8 Å of the inhibitor. The structure was relaxed using the Tripos forcefield keeping the user assigned charges and a constant dielectric of 1000. This dielectric scale allows the retention of electrostatic information but permits breaking of otherwise strong electrostatic interactions as needed. Only the ligand and an 8 Å shell of residues about it were minimized, with the constraint that hinge hydrogen bonds be maintained between 2.5 and 3.2 Å. A harmonic penalty with a constant of 2000 was applied to hinge hydrogen bond distances outside the prescribed range. Minimization terminated at a gradient cutoff of 1 kcal/(mol Å) using BFGS minimization. The resulting structure was then minimized again with all parameters remaining the same as previously noted, except a distance-dependent dielectric of 4 and a gradient cutoff of 0.05 kcal/(mol Å) were used. FlexX¹⁶ with default parameters was then used to confirm that the inhibitor preferred only one binding mode. Models for other compounds could be generated from this final minimized structure by making the appropriate changes to the ligand, followed by minimization similar to above or by docking with FlexX. Surfaces on the site were visualized using the MOLCAD suite in SYBYL with default values.

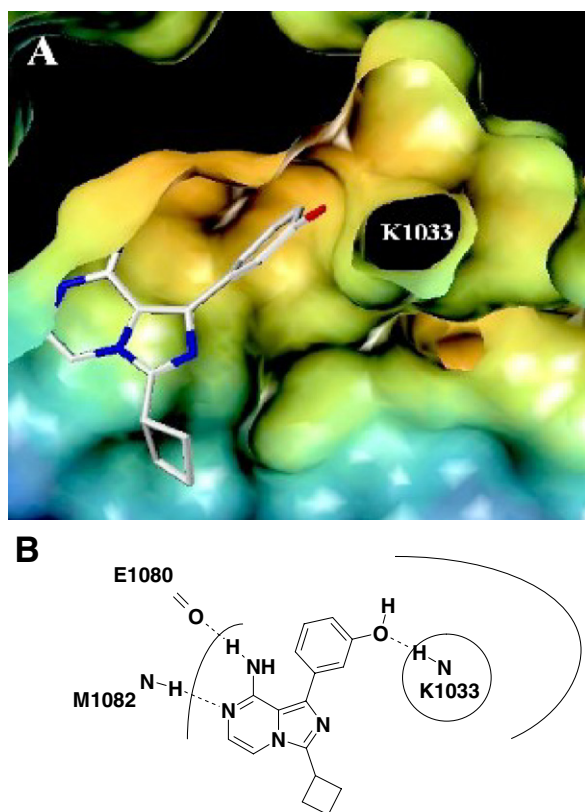
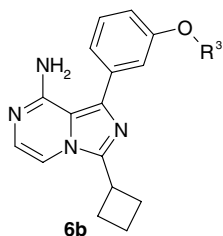


Figure 2. (A) Surface display of a model of the ATP binding pocket with compound **6a.6** bound. The surface is colored by depth from shallow/solvent-exposed blue to deeply buried orange. The hole in the surface is the space carved out by K1033. A small space 'behind' K1033 is visible. (B) 2D representation of Figure 2A, highlighting the key interactions in the site. The basic amine of K1033 makes a key hydrogen bond with the hydroxyl. Canonical hinge binding interactions are also present.

Although the model suggested a small amount of space available behind K1033, toleration of the large 3- and 4-benzyloxy groups on the proximal phenyl ring (compounds **6a.4** and **6a.5**) suggested that a somewhat more sizable non-polar pocket was actually available for binding. Since this pocket is ill-defined in the simple model and the benzyloxy was likely not optimal for the site, further derivatization of the ether tether was undertaken. 3-Hydroxyphenyl-derivative **6a.6** was treated with various alkyl/benzyl halides in the presence of Cs₂CO₃ in DMF to afford a series of alkyl- and benzyl-derived ethers (**6b**), from which a subset of key derivatives are highlighted in Tables 2 and 3. In general, non-polar groups were tolerated, such as compounds **6b.1–6b.4**, while more polar terminal groups such as hydroxyl (**6b.6**), imidazolyl (**6b.7**), and pyrrolidinyl (**6b.8**) were not (Table 2). Interestingly, the 2-pyridyl-methyl moiety was quite well tolerated over that of the 3-pyridyl analog, compounds **6b.9** and **6b.10**, respectively, suggesting a subtle but pronounced difference between the two compounds and their respective interactions with the protein.

With the simple 3-OBn moiety still representing the best proximal phenyl substitution, analoging progressed to establishing an SAR around the benzyl moiety. Of the variety of substituents on the terminal phenyl ring which were explored (Table 3), 2-fluoro (**6c.1**), 2,6-difluoro (**6c.15**), and 2-chloro-6-fluoro (**6c.18**) derivatives

Table 2. IGF-IR biochemical potencies for compounds **6b**

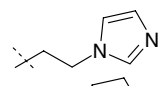
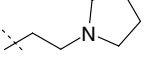
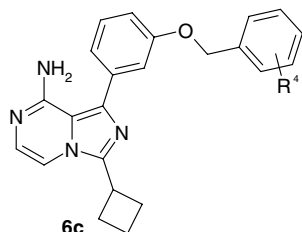
Compound	R ³	IC ₅₀ (μM)
6b.1	Cyclopentyl	3.50
6b.2	Cyclohexyl	1.05
6b.3	–CH ₂ –cyclopropyl	2.27
6b.4	–CH ₂ –cyclohexyl	1.11
6b.5	–CH ₂ CH ₂ OMe	6.28
6b.6	–CH ₂ CH ₂ OH	>10.0
6b.7		>10.0
6b.8		>10.0
6b.9	–CH ₂ –2-pyridyl	1.09
6b.10	–CH ₂ –3-pyridyl	>10.0

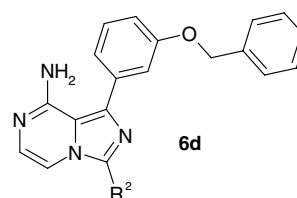
Table 3. IGF-IR biochemical and cell potencies for compounds **6c**

Compound	R ⁴	IC ₅₀ (μM)	
		Biochemical	Cell
6a.4	H	0.606	1.16
6c.1	2-F	0.224	2.06
6c.2	3-F	0.510	3.29
6c.3	4-F	1.23	—
6c.4	2-Cl	0.343	—
6c.5	3-Cl	2.12	—
6c.6	4-Cl	0.980	>10.0
6c.7	2-OCF ₂ H	3.28	—
6c.8	3-OCF ₂ H	5.78	—
6c.9	4-OCF ₂ H	2.82	—
6c.10	2-CN	>10.0	—
6c.11	4-CN	>10.0	—
6c.12	2,3-Difluoro	0.898	5.69
6c.13	3,4-Difluoro	4.48	—
6c.14	2,5-Difluoro	0.329	9.76
6c.15	2,6-Difluoro	0.215	1.59
6c.16	3,5-Difluoro	1.35	—
6c.17	2,6-Dichloro	1.67	—
6c.18	2-Cl,6-F	0.248	2.67
6c.19	3-CHCONH ₂	>10.0	—
6c.20	3-NHCOCH ₃	>10.0	—

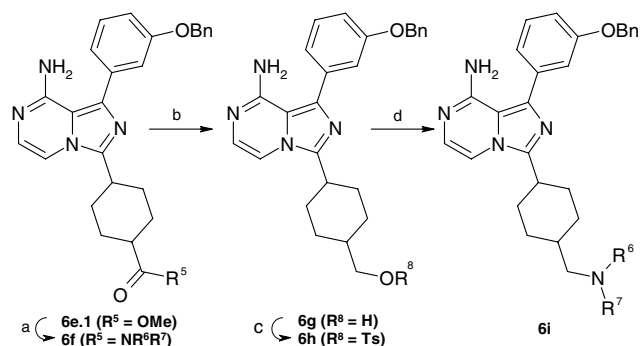
displayed IC₅₀ values below 300 nM, but unfortunately were 10-fold less active in cells. Additionally, a series of polar groups were explored such as amide **6c.19**

(R₄ = 3-CONH₂) and reverse amide **6c.20** (R₄ = 3-NHCOCH₃). As in the 3-pyridyl case (**6b.10**), the general trend suggested that polar substituents at the *meta*-position of the terminal phenyl ring were generally not tolerated in this region of the protein. Additionally, the improved biochemical potency observed with the 2-pyridyl derivative **6b.9** and 2-F derivative **6c.1** suggests that both could be engaging in a hydrogen bonding interaction with the protein.

Structural hypotheses from IGF-IR molecular models suggested that the 8-NH₂ and N7 nitrogen of the imidazopyrazine core were involved in a conventional hinge binding interaction with the protein,¹⁷ and the C3 groups were projecting toward the P-loop, a solvent-exposed region of the protein (Fig. 2). Therefore, a series of compounds was synthesized to explore substituents at position C3 of the imidazopyrazine ring (R²) while maintaining the 3-OBn-phenyl moiety at C1 (Table 4). Cycloalkyl groups other than cyclobutyl such as cyclopentyl and cyclohexyl, **6d.2** and **6d.3**, respectively, were tolerated, as was phenyl (**6d.5**), whereas hydrogen (**6d.6** and **6d.7**) were not tolerated. This suggests that some critical mass at C3 of the imidazopyrazine was required to appropriately interact with the protein. Efforts then focused¹⁸ on further extension towards the solvent-exposed region; C4-cyclohexyl and C3-cyclobutyl substitutions were explored as a follow up to compounds **6d.3** and **6a.4**, respectively. A series of *cis*- and *trans*-amides, as well as aminomethylcyclohexyl derivatives, was synthesized (Scheme 3). Methyl ester **6e.1** was converted to its respective amide **6f** and subsequently reduced to alcohol **6g**. Alcohol **6g** was converted to tosylate **6h**, which was treated with various amines to afford compounds **6i**. In cases **6f** and **6i**, it was determined that the *trans*-isomer was slightly more potent (2- to 3-fold) than the *cis*-isomer (Table 5). In particular, the *trans*-aminomethylcyclohexyl derivatives **6i** displayed IGF-IR kinase inhibition at or below 100 nM and cellular potencies of ~500 nM (**6i.3–6i.5**). General SAR around amides **6f** showed that the tertiary amides were less potent than either the secondary or primary amides, suggesting that the free NH was important for improved

Table 4. IGF-IR biochemical potencies for compounds **6d**

Compound	R ²	IC ₅₀ (μM)
6d.1	H	>10.0
6d.2	Cyclopentyl	1.05
6d.3	Cyclohexyl	3.51
6d.4	Cycloheptyl	3.79
6d.5	Phenyl	1.68
6d.6	1-Naphthyl	>10.0
6d.7	2-Naphthyl	>10.0



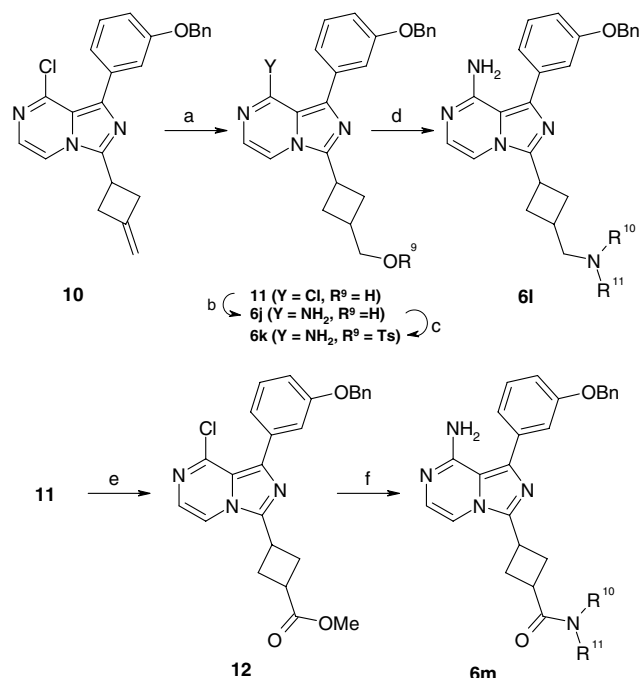
Scheme 3. Reagents and conditions: (a) NaOH to $R^5 = \text{OH}$, then HNR^6R^7 , EDC, HOBT, CH_2Cl_2 or $\text{Al}(\text{CH}_3)_3$, HNR^6R^7 , toluene; (b) LiAlH_4 , THF, rt; (c) Ts_2O , pyridine, THF, -20°C to rt, 16 h; (d) HNR^6R^7 , DIEA, THF, 50°C , 16 h. Compounds **6i.1** and **6i.2** were synthesized via Mitsunobu reaction of respective *cis/trans*-alcohols **6g** with phthalimide followed by treatment with hydrazine.

Table 5. IGF-IR biochemical and cell potencies for compounds **6f** and **6i**

Compound	$R^5/\text{NR}^6\text{R}^7/\text{R}^8$	IC ₅₀ (μM)	
		Biochemical	Cell
6f.1	<i>trans</i> -NH ₂	0.221	0.898
6f.2	<i>cis</i> -NH ₂	0.775	8.57
6f.3	<i>trans</i> -NHMe	0.105	1.72
6f.4	<i>trans</i> -Pyrrolidinyl	1.82	—
6f.5	<i>trans</i> -Piperidinyl	3.40	—
6f.6	<i>trans</i> -NHPH	1.30	—
6f.7	<i>trans</i> -NHBn	1.39	—
6i.1	<i>trans</i> -NH ₂	0.119	0.534
6i.2	<i>cis</i> -NH ₂	0.228	0.560
6i.3	<i>trans</i> -N(Et) ₂	0.115	0.440
6i.4	<i>trans</i> -Azetidiny	0.081	0.398
6i.5	<i>trans</i> -Pyrrolidinyl	0.103	0.547
6i.6	<i>trans</i> -Morpholino	0.091	0.651

efficacy. Moreover, bulkier secondary amides such as compounds **6f.6** and **6f.7** were less potent than the simple methyl amide **6f.3**.

A series of *cis* and *trans*-amido/aminomethylcyclobutyl derivatives was synthesized from 3-methylenecyclobutyl-derived imidazopyrazine intermediate **10** (Scheme 4). Hydroboration of compound **10** with 9-BBN afforded a 5:1 ratio of *cis/trans* alcohols **11**. Ammonolysis of alcohol **11** afforded amine **6j**; the alcohol moiety of compound **6j** was then selectively tosylated to afford a separable mixture of *cis*- and *trans*-tosylates **6k**, which were subsequently treated with a variety of amines to afford compounds such as pyrrolidinyl analogs **6i.1** and **6i.2**. The *cis*-isomer **6i.2** was slightly more potent than its respective *trans*-isomer **6i.1** and, combined with the ease of synthesis, further amino derivatives focused on the *cis*-aminomethylcyclobutyl isomers (**6i.3–6i.8**). The primary amides, **6m**, were synthesized by converting compound **11** to its respective methyl ester followed by treatment with ammonia. Generally, amino derivatives **6i** displayed the best balance of biochemical and cellular potencies (dimethylamino-derivative **6i.4**, cellular IC₅₀ = 191 nM) (Table 6). In both the substituted cyclohexyl and cyclobutyl series, compounds with a higher



Scheme 4. Reagents and conditions: (a) i—0.5 M 9-BBN in THF, 0°C , 16 h; ii—1 N aq NaOH, 30% aq H_2O_2 , 0°C , 30 min; (b) NH_3 , *i*-PrOH, 110°C , 24 h; (c) Ts_2O , pyridine, -20°C , 16 h; (d) $\text{HNR}^{10}\text{R}^{11}$, DIEA, THF, 50°C , 16 h; (e) i— $(\text{COCl})_2$, DMSO, CH_2Cl_2 , -78°C followed by Et_3N quench; ii—NIS, K_2CO_3 , anhyd CH_3OH ; (f) NH_3 , *i*-PrOH, 110°C , 24 h; Amine **6i.3** was synthesized via treatment of *cis*-**6k** with sodium azide followed by hydrogenation over Lindlar's catalyst.

PSA generally displayed a more pronounced biochemical to cellular assay shift in IC₅₀ values. These results are suggestive of poorer cellular permeability, consistent with a PSA >100 Å² of compounds such as amide derivatives **6f.1**, **6f.2**, **6m.1**, and **6m.2**.

For pharmacokinetic evaluation, compound **6a.4** was formulated in 30:70 PEG-400:WFI (water for intravenous injection) and Labrafil® (Gattefosse, France) for oral administration. Compounds **6f.1** and **6i.1** were formulated in 50:50 PEG-400:WFI and 50:50 PEG-400:5% citric acid for oral administration. Female CD-1 mice (6–10 weeks old) received single intravenous doses of 1 mg/kg via tail vein injection and single oral doses of 50 mg/kg by oral gavage. All dose solutions were clear at the time of dosing. Subsequently,

Table 6. IGF-IR biochemical and cell potencies for **6i** and **6m**

Compound	$R^9/\text{NR}^{10}\text{R}^{11}$	IGF-IR IC ₅₀ (μM)	
		Biochemical	Cell
6i.1	<i>trans</i> -Pyrrolidinyl	0.116	0.621
6i.2	<i>cis</i> -Pyrrolidinyl	0.089	0.401
6i.3	<i>cis</i> -NH ₂	0.060	0.690
6i.4	<i>cis</i> -NMe ₂	0.166	0.191
6i.5	<i>cis</i> -Piperidinyl	0.237	0.346
6i.6	<i>cis</i> -Morpholino	0.148	0.658
6i.7	<i>cis</i> -NH <i>i</i> -Pr	0.220	0.376
6i.8	<i>cis</i> -N(Me)-Piperizinyl	0.265	0.758
6m.1	<i>trans</i> -NH ₂	0.526	1.71
6m.2	<i>cis</i> -NH ₂	0.554	2.08

Table 7. PK in mice for compounds **6a.4**, **6f.1**, and **6i.1**

Compound	6a.4	6f.1	6i.1
C_{max} at 50 mg/kg, po (μ M)	0.86	2.22	2.85
AUC _{0–∞} at 50 mg/kg, po (ng h/mL)	1756	1323	3926
Oral bioavailability (%F)	47	34	47
$t_{1/2}$ (h) at 1 mg/kg iv	1.30	0.63	2.29

three animals were sacrificed at designated timepoints, and blood samples were collected in EDTA following cardiac puncture. Following centrifugation at 1500g for 10 min, plasma samples were extracted by protein precipitation with methanol and analyzed by HPLC-MS/MS (PE Sciex API 3000 triple quadrupole mass spectrometer, Applied Biosystems). Drug levels were quantitated against spiked calibration samples prepared in control mouse plasma. Pharmacokinetic parameters were calculated by non-compartmental analysis using the median ($n = 3$) concentration at each timepoint. This analysis showed the compounds to be orally bioavailable with the major parameters presented in Table 7.

In order to determine selectivity of this class of compounds, representative compound **6i.1** was profiled for inhibitory activity against 15 additional purified protein kinases from the tyrosine and serine/threonine kinase families. Protein kinase assays were performed at Upstate Inc. (Charlottesville, VA) by a radiometric method (KinaseProfiler service). Inhibition of protein kinases by compound **6i.1** was assessed at 10 μ M using recombinant purified enzymes in the presence of ATP concentration approximating the respective K_m value for each form of the enzyme. Less than 50% inhibition at 10 μ M of the compound was noted for the following enzymes: Ab1, Cdk2/CyclinA, Cdk2/CyclinE, Chk2, CK2, c-Raf, Fes, IKK- β , MAPK2, p70S6K, PDGFR- β , PDK1, PKA, PKB α , and PKC α . Inhibition of IR was similar to that observed for IGF-IR, reinforcing the high homology between the ATP binding domains of these proteins.

In summary, a series of novel 8-amino-1,3-disubstituted-imidazo[1,5-*a*]pyrazines was designed and synthesized as IGF-IR inhibitors. A combination of systematic medicinal chemistry exploration and modeling-based design-guided modifications of lead compound **6a.4** around the benzyloxy tether, the 8-amino group, and the cycloalkyl moiety at C3 of the imidazopyrazine ring ultimately led to a new series of potent inhibitors, the most interesting of which are the aminomethylcyclohexyl and cyclobutyl analogs (compounds **6i** and **6l**, respectively). Emphasis on addressing the potential metabolic liabilities associated with the benzyloxyphenyl moiety has led our efforts to a search for alternate C1 tethers. In subsequent manuscripts, we will describe the selection of a more constrained quinoline tether, designed through structure-based efforts derived from IGF-IR and IR X-ray co-crystal structures with select imidazopyrazines. In addition, we will discuss efforts to establish selectivity against the highly homologous insulin receptor as well as demonstrate

suitable in vivo PK and PD effects in accordance with tumor growth inhibition.

Acknowledgments

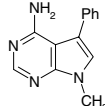
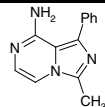
We thank Professor Victor Snieckus for consultation; Ms. Viorica M. Lazarescu and Dr. Minghui Wang for analytical support; Dr. Arno Steinig, Mrs. Yingchuan Sun, and Dr. Jonathan Williams for their synthetic efforts on the 1-(3-benzyloxyphenyl)-imidazo[1,5-*a*]pyrazines series which were not included in this manuscript; and Dr. 's Arlindo Castelhana, Neil Gibson, and Lee Arnold for their managerial support and guidance.

References and notes

- (a) Gschwind, A.; Fischer, O. M.; Ullrich, A. *Nat. Rev. Cancer* **2004**, *4*, 361; (b) Paul, M. K.; Mukhopadhyay, A. K. *Int. J. Med. Sci.* **2004**, *1*, 101; (c) Kumar, C. C.; Madison, V. *Expert Opin. Emerg. Drugs* **2001**, *6*(2), 303; (d) Traxler, P.; Bold, G.; Buchdunger, E.; Caravatti, G.; Furet, P.; Manley, P.; O'Reilly, T.; Wood, J.; Zimmermann, J. *Med. Res. Rev.* **2001**, *21*(6), 499; (e) Noble, M. E. M.; Endicott, J. A.; Johnson, L. N. *Drug Discov.* **2004**, *303*, 1800; (f) Scapin, G. *Drug Discovery Today* **2002**, *7*(11), 601; (g) Sawyer, C. L. *Gene Dev.* **2003**, *17*, 2998; (h) Pollak, M. N.; Schernhammer, E. S.; Hankinson, S. E. *Nat. Rev. Cancer* **2004**, *4*, 505.
- (a) Larsson, O.; Girnita, O.; Girnita, L. *Br. J. Cancer* **2005**, *92*(12), 2097; (b) Pollak, M. N.; Schernhammer, E. S.; Hankinson, S. E. *Nat. Rev. Cancer* **2004**, *4*, 505; (c) Min, Y.; Adachi, Y.; Yamamoto, H.; Ito, H.; Itoh, F.; Lee, C. T.; Nadaf, S.; Carbone, D. P.; Imai, K. *Cancer Res.* **2003**, *63*, 6432; (d) LeRoith, D.; Roberts, C. T., Jr. *Cancer Lett.* **2003**, *195*, 127; (e) Baserga, R.; Peruzzi, F.; Reiss, K. *Int. J. Cancer* **2003**, *106*, 873.
- (a) Wang, Y.; Sun, Y. *Curr. Cancer Drug Targets* **2002**, *2*, 191; (b) Zhang, H.; Yee, D. *Expert Opin. Investig. Drugs* **2004**, *13*, 1569; (c) Quinn, K. A.; Treston, A. M.; Unsworth, E. J.; Miller, M.-J.; Vos, M.; Grimley, C.; Battey, J.; Mulsine, J. L.; Cuttitta, F. *J. Biol. Chem.* **1996**, *271*, 11477; (d) Vella, V.; Pandini, G.; Sciacca, L.; Mineo, R.; Vigneri, R.; Pezzino, V.; Belfiore, A. *J. Clin. Endocrinol. Metab.* **2002**, *87*, 245; (e) Qing, R. Q.; Schmitt, S.; Ruelicke, T.; Stallmach, T.; Schoenle, E. *J. Pediatric Res.* **1996**, *39*, 160; (f) Ma, J.; Pollak, M. N.; Giovannucci, E.; Chan, J. M.; Tao, Y.; Hennekens, C. H.; Stampfer, M. J. *J. Natl. Cancer Inst.* **1999**, *91*(7), 620.
- Zhang, L.; Zhou, W.; Velculescu, V. E.; Kern, S. E.; Hruban, R. H.; Hamilton, S. R.; Vogelstein, B.; Kinzler, K. W. *Science* **1997**, *276*(5316), 1268.
- (a) Resnicoff, M.; Coppola, D.; Sell, C.; Rubin, R.; Ferrone, S.; Baserga, R. *Cancer Res.* **1994**, *54*, 4848; (b) Chernicky, C. L.; Yi, L.; Tan, H.; Gan, S. U.; Ilan, J. *Cancer Gene Ther.* **2000**, *7*, 384.
- (a) Maloney, E. K.; McLaughlin, J. L.; Dagdigian, N. E.; Garrett, L. M.; Connors, K. M.; Zhou, X. M.; Blattler, W. A.; Chittenden, T.; Singh, R. *Cancer Res.* **2003**, *63*, 5073; (b) Wang, Y.; Hailey, J.; Williams, D.; Wang, Y.; Lipari, P.; Malkowski, M.; Wang, X.; Xie, L.; Guanghua, L.; Saha, D.; Ling, W. L. W.; Cannon-Carlson, S.; Greenberg, R.; Ramos, R. A.; Shields, R.; Presta, L.; Brams, P.; Bishop, W. R.; Pachter, J. A. *Mol. Cancer Ther.* **2005**, *4*, 1214; (c) Cohen, B. D.; Baker, D. A.; Soderstrom, C.; Tkalecic, G.; Rossi, A. M.; Miller, P. E.; Tengowski, M. W.;

- Wang, F.; Gualberto, A.; Beebe, J. S.; Moyer, J. D. *Clin. Cancer Res.* **2005**, *11*(5), 2063; (d) Goetsch, L.; Gonzalez, A.; Leger, O.; Beck, A.; Pauwels, P. J.; Haeuw, J. F.; Corvaia, N. *Int. J. Cancer* **2005**, *113*(2), 316.
7. (a) Prager, D.; Li, H. L.; Asa, S.; Melmed, S. *Proc. Natl. Acad. Sci. U.S.A.* **1994**, *91*, 2181; (b) Kalebic, T.; Blakesley, V.; Slade, C.; Plasschaert, S.; Leroith, D.; Melman, L. J. *Int. J. Cancer* **1998**, *76*, 223; (c) Scotlandi, K.; Avnet, S.; Benini, S.; Manara, M. C.; Serra, M.; Cerisano, V.; Perdichizzi, S.; Lollini, P. L.; De Giovanni, C.; Landuzzi, L.; Picci, P. *Int. J. Cancer* **2002**, *101*, 11.
8. (a) Garcia-Echeverria, C.; Pearson, M. A.; Marti, A.; Meyer, T.; Mestan, J.; Zimmermann, J.; Gao, J.; Brueggen, J.; Capraro, H.-G.; Cozens, R.; Evans, D. B.; Fabbro, D.; Furet, P.; Porta, D. G.; Liebetanz, J.; Martiny-Baron, G.; Ruetz, S.; Hofmann, F. *Cancer Cell* **2004**, *5*, 231; (b) Haluska, P.; Carboni, J. M.; Loegering, D. A.; Lee, F. Y.; Wittman, M.; Saulnier, M. G.; Frennesson, D. B.; Kalli, K. R.; Conover, C. A.; Attar, R. M.; Kaufmann, S. H.; Gottardis, M.; Erlichman, C. *Cancer Res.* **2006**, *66*, 362; (c) Girnita, A.; Girnita, L.; Prete, F.-D.; Bartolazzi, A.; Larsson, O.; Axelson, M. *Cancer Res.* **2004**, *64*, 236; (d) Li, W.; Favellyukis, S.; Yang, J.; Zeng, Y.; Yu, J.; Gangjee, A.; Miller, W. T. *Biochem. Pharmacol.* **2004**, *68*, 145.
9. (a) Garcia-Echeverria, C. *IDRUGS* **2006**, *9*(6), 415; (b) Surmacz, E. *Oncogene* **2003**, *22*, 6589.
10. (a) Dai, Y.; Guo, Y.; Frey, R. R.; Ji, Z.; Curtin, M. L.; Ahmed, A. A.; Albert, D. H.; Arnold, L.; Arries, S. S.; Barlozzari, T.; Bauch, J. L.; Bouska, J. J.; Bousquet, P. F.; Cunha, G. A.; Glaser, K. B.; Guo, J.; Li, J.; Marcotte, P. A.; Marsh, K. C.; Moskey, M. D.; Pease, L. J.; Stewart, K. D.; Stoll, V. S.; Tapang, P.; Wishart, N.; Davidsen, S. K.; Michaelides, M. R. *J. Med. Chem.* **2005**, *48*, 6066; (b) Burchat, A. F.; Calderwood, D. J.; Friedman, M. M.; Hirst, G. C.; Li, B.; Rafferty, P.; Ritter, K.; Skinner, B. S. *Bioorg. Med. Chem. Lett.* **2002**, *12*, 1687; (c) Calderwood, D. J.; Johnston, D. N.; Munschauer, R.; Rafferty, P. *Bioorg. Med. Chem. Lett.* **2002**, *12*, 1683; (d) Missbach, M.; Altmann, E.; Widler, L.; Šušar, M.; Buchdunger, E.; Mett, H.; Meyer, T.; Green, J. *Bioorg. Med. Chem. Lett.* **2000**, *10*, 945; (e) Widler, L.; Green, J.; Missbach, M.; Šušar, M.; Altmann, E. *Bioorg. Med. Chem. Lett.* **2001**, *11*, 849; (f) Altmann, E.; Missbach, M.; Green, J.; Šušar, M.; Wagenknecht, H.-A.; Widler, L. *Bioorg. Med. Chem. Lett.* **2001**, *11*, 853; (g) Arnold, L.; Calderwood, D. J.; Dixon, R. W.; Johnston, D. N.; Kamens, J. S.; Munschauer, R.; Rafferty, P.; Ratnofsky, S. E. *Bioorg. Med. Chem. Lett.* **2000**, *10*, 2167; (h) Burchat, A. F.; Calderwood, D. J.; Hirst, G. C.; Holman, N. J.; Johnston, D. N.; Munschauer, R.; Rafferty, P.; Tometzki, G. B. *Bioorg. Med. Chem. Lett.* **2000**, *10*, 2171.

11. (a) Predicted physicochemical properties of imidazo[1,5-*a*]pyrazine and pyrrolo[2,3-*d*]pyrimidine

Compound	PSA (Å)	AlogP	-LogS
	56.7	2.06	3.67
	56.2	1.44	2.76

- Polar surface area calculated according to method in (b) Ertl, P.; Rohde, B.; Selzer, P. *J. Med. Chem.* **2000**, *43*, 3714; AlogP calculated according to method in (c) Ghose, A. K.; Viswanadhan, V. N.; Wendoloski, J. J. *J. Phys. Chem. A* **1998**, *102*, 3762; Maximal solubility, S (in Molar), calculated according to method in (d) Tetko, I. V.; Tanchuk, V. Y.; Kasheva, T. N.; Villa, A. E. *J. Chem. Inf. Comput. Sci.* **2001**, *41*, 1488.
12. Beck, P.A.; Cesario, C.; Cox, M.; Dong, H.-Q.; Foreman, K.; Mulvihill, M. J.; Nigro, A. I.; Saroglou, L.; Steinig, A. G.; Sun, Y.; Weng, Q.; Werner, D.; Wilkes, R.; Williams, J.U.S. Pat. Appl. 2006084654 A1.
13. (a) Turck, A.; Mojovic, L.; Queguiner, G. *Synthesis* **1988**, *11*, 881; (b) Ple, N.; Turck, A.; Heynderickx, A.; Queguiner, G. *Tetrahedron* **1998**, *54*, 9701.
14. (a) The coordinates for chain 'A' were extracted from the file associated with pdb identifier '1JQH'; (b) Berman, H. M.; Westbrook, J.; Feng, Z.; Gilliland, G.; Bhat, T. N.; Weissig, H.; Shindyalov, I. N.; Bourne, P. E. *Nucleic Acids Res.* **2000**, *28*, 235.
15. Case, D. A.; Pearlman, D. A.; Caldwell, J. W.; Cheatham, T. E., III; Wang, J.; Ross, W. S.; Simmerling, C. L.; Darden, T. A.; Merz, K. M.; Stanton, R. V.; Cheng, A. L.; Vincent, J. J.; Crowley, M.; Tsui, V.; Gohlke, H.; Radmer, R. J.; Duan, Y.; Pitera, J.; Massova, I.; Seibel, J. L.; Singh, U. C.; Weiner, P. K.; Kollman, P. A. *AMBER 7*; University of California: San Francisco, 2002.
16. Rarey, M.; Kramer, B.; Lengauer, T.; Klebe, G. *J. Mol. Biol.* **1996**, *261*, 470.
17. Consistent with this structural hypothesis, substituents on the 8-amino moiety such as methyl, ethyl, phenyl, benzyl or acyl proved detrimental (>10 μ M) to IGF-IR activity as expected (data not shown).
18. Despite its potency, phenyl derivative **6d.5** was not pursued further in order to avoid incorporating a third phenyl group into the molecule and therefore, additional potential sites of metabolism.